


## Article

# A Joint State-Parameter Identification Algorithm of a Structure with Non-Diagonal Mass Matrix Based on UKF with Unknown Mass

Shiyu Wang and Ying Lei \* 

School of Architecture and Civil Engineering, Xiamen University, Xiamen 361005, China; kaixing007wang@126.com

\* Correspondence: ylei@xmu.edu.cn

**Abstract:** Inaccurate mass estimates have been recognized as an important source of uncertainty in structural identification, especially for large-scale structures with old ages. Over the past decades, some identification algorithms for structural states and unknown parameters, including unknown mass, have been proposed by researchers. However, most of these identification algorithms are based on the simplified mechanical model of chain-like structures. For a chain-like structure, the mass matrix and its inverse matrix are diagonal matrices, which simplify the difficulty of identifying the structure with unknown mass. However, a structure with a non-diagonal mass matrix is not of such a simple characteristic. In this paper, an online joint state-parameter identification algorithm based on an Unscented Kalman filter (UKF) is proposed for a structure with a non-diagonal mass matrix under unknown mass using only partial acceleration measurements. The effectiveness of the proposed algorithm is verified by numerical examples of a beam excited by wide-band white noise excitation and a two-story one-span plane frame structure excited by filtered white noise excitation generated according to the Kanai–Tajimi power spectrum. The identification results show that the proposed algorithm can effectively identify the structural state, unknown stiffness, damping and mass parameters of the structures.

**Keywords:** unknown mass; joint state-parameter identification; non-diagonal mass matrix; partial acceleration measurement



**Citation:** Wang, S.; Lei, Y. A Joint State-Parameter Identification Algorithm of a Structure with Non-Diagonal Mass Matrix Based on UKF with Unknown Mass. *Buildings* **2022**, *12*, 826. <https://doi.org/10.3390/buildings12060826>

Academic Editors: Zhiming Zhang, Mingming Song and Qipei (Gavin) Mei

Received: 6 May 2022  
Accepted: 10 June 2022  
Published: 14 June 2022

**Publisher's Note:** MDPI stays neutral with regard to jurisdictional claims in published maps and institutional affiliations.



**Copyright:** © 2022 by the authors. Licensee MDPI, Basel, Switzerland. This article is an open access article distributed under the terms and conditions of the Creative Commons Attribution (CC BY) license (<https://creativecommons.org/licenses/by/4.0/>).

## 1. Introduction

Nowadays, more and more large-scale civil building structures, especially high-rise buildings and long-span bridges, are being built all over the world. Once these structures are constructed and used, functional degradation of the structures will become a concerning issue as the working-age of these structures increases. In order to ensure the safety and reliability of these structures, it is particularly important to obtain the information on the state and parameters of these structures accurately and timely. Structural health monitoring (SHM) has received increasing attention in recent decades with the increasing demand for effectively managing the health condition of these important infrastructures. Structural identification (SI) methods play key roles in structural damage detection, model updating and performance evaluation, which are the most important parts of structural health monitoring. Therefore, the proposal of efficient and reliable structural system identification algorithms is very important for the evaluation of the working performance of the structure and the assessment of post-event conditions after natural disasters.

Over the past decades, a great deal of research has been conducted for structural identification in either the frequency domain [1–5] or the time domain [6–10]. It should be noted that almost all of the studies reviewed above assume that structural mass is known when structural systems are identified. In practice, it is often difficult or even impossible to obtain a priori information about the mass of an engineering structure in

service. The inaccurate structural mass estimation causes large errors in the identification of the structure, which endanger the reliability and even the safety of the structure.

In order to deal with this problem, many researchers developed some system identification algorithms under unknown mass. These system identification algorithms can be roughly divided into two categories, namely, the frequency-domain method and the time-domain method. In the frequency-domain system identification algorithm, Yuan et al. [11] proposed an iterative algorithm for identifying structural mass and stiffness matrix elements of chain-like structures based on the first two orders of structural mode measurement by combining modal expansion with the least-squares algorithm. Chakraverty et al. [12] refined the above method by using Holzer criteria to improve its computational efficiency and accuracy. Then, Mukhopadhyay et al. [13,14] also proposed a stiffness and mass matrix identification method based on modal expansion. However, in order to perform modal mass normalization processing, the structural mass, which the sensor is installed, must be known prior. In addition, a flexibility-based damage identification algorithm that does not require knowledge of structural mass is provided by Zhang et al. [15]. Farshadi et al. [16] developed a (Transfer ratio function) FRF-based finite element (FE) model updating algorithm. In this algorithm, the sensitivity equation between frequency response function and parameter change is constructed, and the change in stiffness and mass are identified by solving the equation. The above algorithms are all deterministic algorithms that cannot quantitatively describe the uncertainty of identified results. The Bayesian statistical probabilistic approach provides a method that can not only provide us with an optimal estimate of the state and parameters of a structural system but also quantitatively describe the uncertainty of this estimate. Mustafa et al. [17] proposed an efficient and robust Bayesian model updating to update mass and stiffness by introducing a new objective function to remove the coupling effect of stiffness and mass matrix to solve the unidentifiable problem of the traditional Bayesian method when stiffness and mass matrix identified simultaneously. Furthermore, Kim et al. [18] proposed a novel Bayesian model updating algorithm. In the algorithm, the additional mass or additional stiffness is added to the structure to decouple the coupling effects of mass and stiffness matrices of the identification algorithm so that the model mass and stiffness parameters can be updated by comparing the measured data of the reference model and the modified model.

On the other hand, various time-domain techniques were developed. Mei et al. [19] proposed an algorithm synthesis of the Auto-Regressive Moving Average model and structural dynamics equations to identify the changes in structural element mass and stiffness. However, in this algorithm, only one damage index is defined, so it cannot identify the changes in mass and stiffness simultaneously. The algorithm above is improved by Do et al. [20] by introducing two damage indicators for identifying the changes in the stiffness and mass in identifying the structure simultaneously. A restoring force identification method is provided by Marsi et al. [21] to identify chain-like dynamic structural systems under unknown mass. Based on his work, a time-domain identification algorithm of modal parameters to handle the case of chain-like dynamic systems with unknown ambient excitation under unknown mass was proposed by Nayeri et al. [22]. However, this algorithm can only identify the stiffness and mass coupling coefficients of the structure. Zhan et al. [23] generalized the approach by introducing the clustering algorithm to decouple the stiffness and mass coupling coefficients. Meanwhile, Nayeri et al. [24] provided an algorithm combining natural excitation technology and eigenvalue realization technology to identify the modal parameters of structures with unknown mass. Xu et al. [25] investigated a time-domain algorithm for simultaneous identification of mass and nonlinear restoring force based on the least square algorithm and verified the algorithm with a chain-like nonlinear structure of six degrees of freedom with a Magnetorheological (MR) damper mounted in the middle. Huang et al. [26] employed the Kalman filter (KF) technique together with energy equilibrium equations to develop a method that can identify the damping, stiffness and mass of the structure simultaneously online. However, these time-domain algorithms mentioned above all need to be employed under the condition of full measurement of structural

acceleration, which may have limited the application of the algorithms. In order to address the aforementioned issues, an adaptive Extended Kalman Filter (EKF) was proposed by Reina et al. [27] to perform joint time-varying mass and state estimation for vehicles, which is simplified to a single degree of freedom model under partial acceleration measurements. Boada et al. [28] proposed a real-time locomotive Vehicle and Road Irregularities estimation algorithm based on dual KF simultaneously. In the dual KF, the first KF is used to estimate the Vehicle state, and the latter is used for mass estimation. Lei et al. [29] extended the method of Zhan et al. [25] by introducing EKF to replace the least squares to identify the mass stiffness coupling parameters to identify structural stiffness and mass changes in the case of partial acceleration response measurement. Zhang et al. [30,31] proposed a loop substructure identification method for chain-like structures, which can identify the mass and stiffness parameters of selected substructures under partial acceleration measurements. Then, Xu et al. [32] also investigated a method for the identification of nonlinearity restoring force of chain-like structural and mass simultaneously using partial acceleration measurements. However, the application of EKF with weighted global iteration (EKF-WGI) makes it impossible to implement the algorithm online.

It is noted that most of the methods reviewed in the aforementioned literature are only suitable for chain-like structures, in which both the mass matrix and the inverse matrix are diagonal matrices. This characteristic of a mass matrix for the chain-like structure greatly reduces the difficulty of structure identification under unknown mass. However, many civil structures cannot simply be simulated by a chain-like structure model, such as super high-rise frame shear wall structures, long-span bridges and industrial plants. To the best of the authors' knowledge, there are very limited studies on joint state-parameter identification algorithms of non-chain-like structures under unknown mass. The joint state-parameters identification, even for linear structure, is essentially a nonlinear problem due to the coupling effects between unknown structural parameters and unknown state variables. Compared with other schemes based on the nonlinear Kalman framework (e.g., EKF, particle filter (PF)), which can identify nonlinear systems, UKF becomes a better choice because it does not need to calculate the Jacobian matrix and has high computational efficiency. To this end, this paper provided an online joint state-parameter identification algorithm of a non-chain-like structure based on UKF under unknown mass using only partial acceleration responses. The content of the paper is organized as follows: Section 2 briefly introduces the calculation process of UKF; Section 3 includes two numerical simulation cases in the context of the beam-type model and plane-frame model used to assess the performance of the joint state-parameter identification algorithm of a non-chain-like structure under unknown mass. Finally, the conclusion and further research are given in the conclusions section.

## 2. Brief Review of the Unscented Kalman Filter

A generalized  $n$ -DOF structural system dynamics equation can be expressed as

$$\mathbf{M}\ddot{\mathbf{z}} + \mathbf{F}(\mathbf{z}, \dot{\mathbf{z}}, \boldsymbol{\theta}) = \boldsymbol{\eta}\mathbf{f} \quad (1)$$

In which  $\mathbf{M}$  is the mass matrix;  $\mathbf{z}$ ,  $\dot{\mathbf{z}}$  and  $\ddot{\mathbf{z}}$  are  $n$ -dimension vectors of displacement, velocity and acceleration, respectively;  $\mathbf{F}(\mathbf{z}, \dot{\mathbf{z}}, \boldsymbol{\theta})$  is a generalized restoring force equation vector;  $\boldsymbol{\theta}$  is a  $q$ -dimension structural parametric vector containing the parameters that need to parameterize the restoring force function  $\mathbf{F}(\mathbf{z}, \dot{\mathbf{z}}, \boldsymbol{\theta})$ ;  $\boldsymbol{\theta}_m$  is an  $l$ -dimension vector that to be identified in this study, which includes the structural mass.  $\mathbf{f}$  is a  $p$ -dimension external excitation vector and  $\boldsymbol{\eta}$  is the influence matrix corresponding to  $\mathbf{f}$ . Since the structural system in this paper is a time-invariant system, the time derivatives of unknown parameters in the structure  $\dot{\boldsymbol{\theta}}_{m(i)} = 0 (i = 1, 2, 3, \dots, l)$ . An augmented state vector is defined as  $\mathbf{X} = \{\mathbf{X}_z^T, \boldsymbol{\theta}_m^T\}^T = \{\mathbf{z}^T, \dot{\mathbf{z}}^T, \boldsymbol{\theta}_m^T\}^T$ , which includes structural displacement, velocity

and unknown structural parameters, including the structural mass, stiffness and damping coefficients. The state-space form of Equation (1) can be expressed as follows:

$$\dot{\mathbf{X}} = \begin{Bmatrix} \dot{\mathbf{X}}_z \\ \dot{\boldsymbol{\theta}}_m \end{Bmatrix} = \begin{Bmatrix} \dot{\mathbf{z}} \\ \dot{\boldsymbol{\theta}}_m \end{Bmatrix} = \begin{Bmatrix} \dot{\mathbf{z}} \\ \mathbf{M}^{-1}[\boldsymbol{\eta}\mathbf{f} - \mathbf{F}(\mathbf{z}, \dot{\mathbf{z}}, \boldsymbol{\theta})] \\ 0 \end{Bmatrix} = \mathbf{g}(\mathbf{X}, \mathbf{f}) \quad (2)$$

where  $\mathbf{g}(\cdot)$  denotes system equations for the structural system.

The continuous system Equation (2) on the  $k$ th time step can be discrete to be the following form:

$$\mathbf{X}_{k+1} = \mathbf{X}_k + \int_{k\Delta t}^{(k+1)\Delta t} \mathbf{g}(\mathbf{X}_{t|k}, \mathbf{f}_k) dt \quad (3)$$

The observation equations for the structural system can be formulated as

$$\mathbf{y}_{k+1} = \mathbf{h}(\mathbf{X}_{k+1}, \mathbf{f}_{k+1}) + \mathbf{v}_{k+1} \quad (4)$$

where  $\mathbf{y}_{k+1}$  is an  $m$ -dimension measurement vector at time  $t = (k+1)\Delta t$  with  $\Delta t$  being the sampling time step, and  $\mathbf{v}_{k+1}$  is the measurement noise vector modeled as Gaussian white noise with zero mean and a covariance matrix  $\mathbf{E}(\mathbf{v}_{k+1}\mathbf{v}_{k+1}^T) = \mathbf{R}_{k+1}$ .

The unscented Kalman filter is implemented in the following three steps:

(1) Sigma point generation step

Firstly, a set of  $2N + 1$  sigma points whose mean and covariance are  $\mathbf{X}_{k|k}$  and  $\mathbf{P}_{k|k}^{\mathbf{XX}}$ , respectively, are reproduced as

$$\mathbf{X}_{i,k|k} = \begin{cases} \mathbf{X}_{k|k} & , i = 0 \\ \mathbf{X}_{k|k} + (\sqrt{(N+\lambda)\mathbf{P}_{k|k}^{\mathbf{XX}}})_i & , i = 1, \dots, N \\ \mathbf{X}_{k|k} - (\sqrt{(N+\lambda)\mathbf{P}_{k|k}^{\mathbf{XX}}})_i & , i = N+1 \dots 2N \end{cases} \quad (5)$$

where  $N$  is defined as the dimension of the state vector  $\mathbf{X}$ ,  $\mathbf{X}_{k|k} = \mathbf{E}\{\mathbf{X}_k\}$ ,  $\mathbf{P}_{k|k}^{\mathbf{XX}} = \mathbf{E}\{(\mathbf{X}_k - \mathbf{X}_{k|k})(\mathbf{X}_k - \mathbf{X}_{k|k})^T\}$ ,  $(\sqrt{(N+\lambda)\mathbf{P}_{k|k}^{\mathbf{XX}}})_i$  denotes the  $i$ th column of the matrix square root,  $\lambda = \alpha^2(N + \kappa) - N$  is a scaling parameter,  $\alpha$  is a scaling parameter used to incorporate higher-order information. It is often set to an extremely small positive value (e.g.,  $2 \times 10^{-3}$ );  $\kappa$  is a secondary scaling parameter.

(2) The time updating step

The sigma points are propagated by structural system dynamic Equations as follows:

$$\mathbf{X}_{i,k+1|k} = \mathbf{X}_{i,k|k} + \int_{k\Delta t}^{(k+1)\Delta t} \mathbf{g}(\mathbf{X}_{t|k}, \mathbf{f}_k) dt \quad (6)$$

and the a priori estimate of the state vector  $\mathbf{X}_{k+1|k}$  and corresponding error covariance matrix  $\mathbf{P}_{k+1|k}^{\mathbf{XX}}$  are calculated as

$$\mathbf{X}_{k+1|k} = \sum_{i=0}^{2N} w_i^{(m)} \mathbf{X}_{i,k+1|k} \quad (7)$$

$$\mathbf{P}_{k+1|k}^{\mathbf{XX}} = \sum_{i=0}^{2N} w_i^{(c)} (\mathbf{X}_{i,k+1|k} - \mathbf{X}_{k+1|k})(\mathbf{X}_{i,k+1|k} - \mathbf{X}_{k+1|k})^T + \mathbf{Q}_{k+1} \quad (8)$$

where  $w_i^{(m)}$  and  $w_i^{(c)}$  are the weights for the predicted mean and covariance, respectively, and given by

$$w_0^{(m)} = \frac{\lambda}{N+\lambda}; w_0^{(c)} = \frac{\lambda}{N+\lambda} + (1 - \alpha^2 + \beta); \quad (9a)$$

$$w_i^{(m)} = w_i^{(c)} = \frac{\lambda}{2(N + \lambda)} \quad (i = 1, 2 \dots 2N) \quad (9b)$$

where  $\beta$  is a parameter used to contain prior information of the distribution of state variables, and for Gaussian distribution,  $\beta = 2$  is optimal.

The predicted measurement  $\mathbf{y}_{k+1|k}$  and its error covariance matrix  $\mathbf{P}_{k+1|k}^{yy}$  is computed as

$$\mathbf{y}_{i,k+1|k} = h(\chi_{i,k+1|k}, \mathbf{f}_{k+1}); \quad \mathbf{y}_{k+1|k} = \sum_{i=0}^{2N} w_i^{(m)} \mathbf{y}_{i,k+1|k} \quad (10)$$

$$\mathbf{P}_{k+1|k}^{yy} = \sum_{i=0}^{2N} w_i^{(c)} (\mathbf{y}_{i,k+1|k} - \mathbf{y}_{k+1|k}) (\mathbf{y}_{i,k+1|k} - \mathbf{y}_{k+1|k})^T + \mathbf{R}_{k+1} \quad (11)$$

and the cross-covariance  $\mathbf{P}_{k+1|k}^{Xy}$  matrix is calculated as

$$\mathbf{P}_{k+1|k}^{Xy} = \sum_{i=0}^{2N} w_i^{(c)} (\mathbf{x}_{i,k+1|k} - \mathbf{X}_{k+1|k}) (\mathbf{y}_{i,k+1|k} - \mathbf{y}_{k+1|k})^T \quad (12)$$

(3) The measurement updating step

Finally, the augmented state vector  $\mathbf{X}_{k+1|k+1}$  and error covariance matrix  $\mathbf{P}_{k+1|k+1}^{XX}$  are updated with the measured output using the Kalman filtering Equations

$$\mathbf{X}_{k+1|k+1} = \mathbf{X}_{k+1|k} + \mathbf{K}_m (\mathbf{y}_{k+1} - \mathbf{y}_{k+1|k}) \quad (13)$$

$$\mathbf{P}_{k+1|k+1}^{XX} = \mathbf{P}_{k+1|k}^{XX} - \mathbf{K}_m \mathbf{P}_{k+1|k}^{yy} \mathbf{K}_m^T \quad (14)$$

in which is the Kalman gain matrix  $\mathbf{K}_{k+1}$  given by

$$\mathbf{K}_{k+1} = \mathbf{P}_{k+1|k}^{Xy} (\mathbf{P}_{k+1|k}^{yy})^{-1} \quad (15)$$

By implementing the identification algorithm based on the unscented Kalman filter, the augmented state vector of the structural system, which contains unknown structural parameters including structural mass, stiffness and damping coefficients, can be identified.

### 3. Numerical Validation

In this section, two numerical simulation cases are given aimed at verifying the effectiveness of the UKF algorithm for joint state-parameter identification of a structure with a non-diagonal mass matrix under unknown mass in the context of two types of non-chain-like structural models: beam-type model and plan-frame model.

#### 3.1. Identification of a Beam-Type Structure Subjected to White Noise Excitation

Considering only chain-like structures were used to identify stiffness, damping and mass simultaneously in most previous studies, a beam-type structure is investigated in this case. The structure under consideration is a simply supported Euler beam, shown in Figure 1. The beam is modeled using a two-dimensional finite element (FE) model and is equally discretized into six beam elements. For these Euler beam elements, only bending deformations in the vertical plane are considered, and shear deformations are ignored since the shear deformations are very small as compared to the bending deformations. The beam model contains a total of 12 DOFS, which includes five vertical DOFS and seven rotational DOFS.

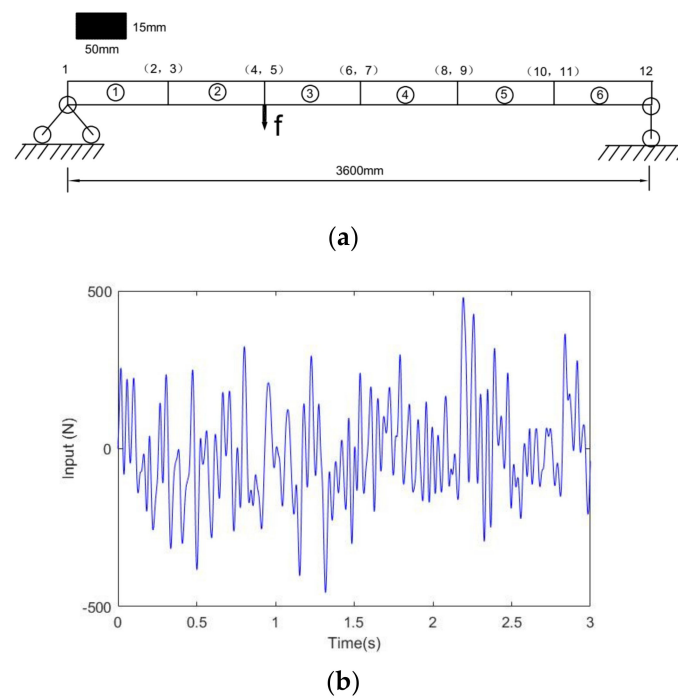


**Figure 1.** A simply supported beam subjected to white noise excitation. (a) A simply supported beam with unknown parameters; (b) broadband white noise excitation.

The beam elements adopt a consistent mass matrix and consistent stiffness matrix. Let  $\mathbf{M}_i$  and  $\mathbf{K}_i$  be the mass matrix and stiffness matrix of the  $i$ -th beam element in the element local coordinate, respectively. The local beam elemental consistent mass and consistent stiffness matrices are calculated using the cubic interpolation functions. The interpolation functions of the  $i$ -th element in its local coordinate can be obtained as follows:

$$\mathbf{H}_i = \left\{ 1 - 3\left(\frac{x}{l_i}\right)^2 + 2\left(\frac{x}{l_i}\right)^3, x - 2l_i\left(\frac{x}{l_i}\right)^2 + l_i\left(\frac{x}{l_i}\right)^3, 3\left(\frac{x}{l_i}\right)^2 - 2\left(\frac{x}{l_i}\right)^3, -l_i\left(\frac{x}{l_i}\right)^2 + l_i\left(\frac{x}{l_i}\right)^3 \right\} \quad (16)$$

where  $l_i$  is the length of the  $i$ -th beam element. The local mass and stiffness matrices for the  $i$ -th beam element are provided in Appendix A.

The equation of motion for the simply supported beam can be given by:

$$\mathbf{M}_b \ddot{\mathbf{z}} + \mathbf{C}_b \dot{\mathbf{z}} + \mathbf{K}_b \mathbf{z} = \boldsymbol{\eta} \mathbf{f} \quad (17)$$

where  $\ddot{\mathbf{z}}$ ;  $\dot{\mathbf{z}}$ ;  $\mathbf{z}$  are the acceleration, velocity and displacement responses of the simply supported beam, respectively.  $\mathbf{f}$  is a one-dimension external excitation vector and  $\boldsymbol{\eta}$  is the influence matrix corresponding to  $\mathbf{f}$ .

$\mathbf{M}_b$  and  $\mathbf{K}_b$  are the global mass and stiffness matrices of the simply supported beam, respectively, which can be obtained as the assembly of local element mass and local stiffness matrices. For the simply supported beam, the Rayleigh damping is assumed, and the global damping matrix  $\mathbf{C}_b$  is expressed as:

$$\mathbf{C}_b = a_1 \mathbf{M}_b + a_2 \mathbf{K}_b \quad (18)$$

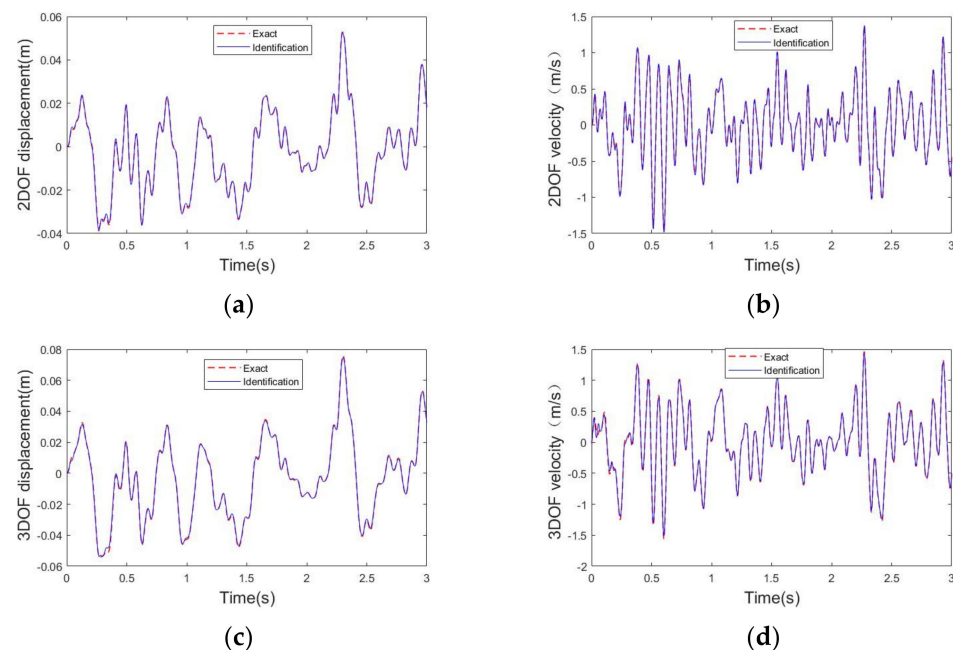
where  $a_1$  and  $a_2$  are the damping coefficients. The mass, stiffness and damping coefficients are considered unknown in this example. The state vector  $\mathbf{X}_z$  and parameter vector  $\boldsymbol{\theta}_m$  of the structural system are combined to form the augmented state vector  $\mathbf{X} = [\mathbf{z}^T, \dot{\mathbf{z}}^T, \bar{\mathbf{m}}^T, \mathbf{k}^T, a_1, a_2]^T$ .

In this case, the length of the beam is 3.6 m, and the whole beam adopts a rectangular section with a uniform section size with a width of 50 mm and a height of 15 mm. The

Young's modulus and material density of the beam is chosen as 206 GPa and 7850 kg/m<sup>3</sup>, respectively. The first two natural frequencies obtained from the beam model are 21.4 Hz and 133.7 Hz; a modal damping ratio of 5% is assumed for the first two modes.

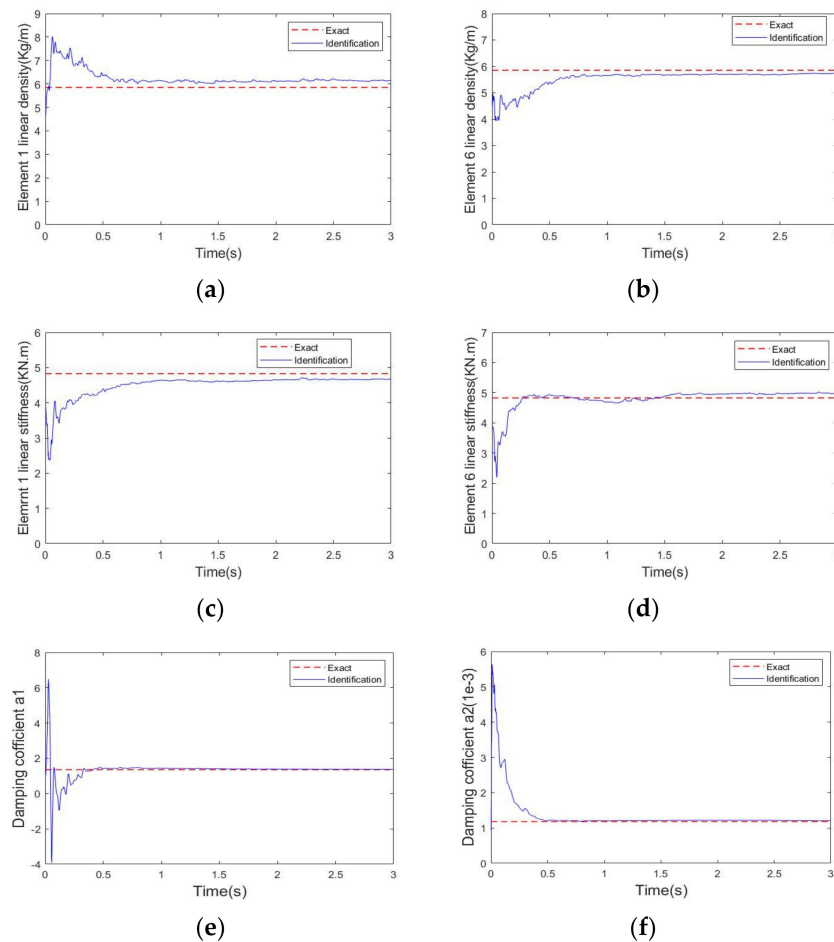
Structural parameters are selected as follows: The cross-sectional area and moment of inertia of each beam element are  $A_i = 7.5 \times 10^{-4} \text{ m}^2$  and  $I_{zi} = 1.406 \times 10^{-8} \text{ m}^4$  ( $i = 1, 2 \dots 6$ ), respectively. The linear stiffness of each beam element is defined as  $k_i = \frac{EI_{zi}}{l_i} = 4.828 \text{ KN.m}$ ; the linear mass density of each element is defined as  $\bar{m}_i = \rho_i A_i = 5.85 \text{ kg/m}$  ( $i = 1, 2 \dots 6$ ). The Rayleigh damping coefficients were calculated to be  $a_1 = 1.356$  and  $a_2 = 1.179 \times 10^{-3}$  according to the first two nature frequencies. The initial guess values for the unknown parameters are selected as:  $\bar{m}_{i,0} = 4.68 \text{ kg/m}$ ,  $k_{i,0} = 3.862 \text{ KN.m}$  ( $i = 1, 2 \dots 6$ ),  $a_{1,0} = 1.084$ ,  $a_{2,0} = 0.944 \times 10^{-3}$ . The external excitation acting on a simply supported beam is assumed to be broadband white noise, which acts on the 4th DOF. From the finite element model built in matlab, the acceleration, velocity and displacement responses of the structure are obtained by solving differential Equation (17) using the 4th-order Ronge–Kutta integration method. Only five accelerometers are deployed at the 2nd, 4th, 6th, 8th and 10th DOFs, respectively, to measure the vertical accelerations. When considering the existence of measurement noise, a Gaussian white sequence with a 1% root-mean-square noise-to-signal ratio is added to the calculated response. The sampling frequency is 1000 Hz, and the sampling time is 3 s.

Figure 2 shows the comparisons of the identified and exact time histories of vertical displacement of nodal 2 ( $z_2$ ), vertical velocity of nodal 2 ( $\dot{z}_2$ ), rotational displacement of nodal 2 ( $z_3$ ) and rotational velocity of nodal 2 ( $\dot{z}_3$ ) obtained from the simulation case. It is shown that both structural displacement and velocity responses can be well tracked.



**Figure 2.** Comparisons of the exact and identified displacements and velocities. (a) Comparison of the exact and identified; (b) comparison of the exact and identified; (c) comparison of the exact and identified; (d) comparison of the exact and identified.

The convergence of six unknown parameters ( $\bar{m}_1, \bar{m}_6, k_1, k_6, a_1, a_2$ ) from the numerical case above was demonstrated in Figure 3. It can be noticed that these identified parameter values can converge to their exact values quite fast.



**Figure 3.** Parameter estimation results for the simply supported beam. (a) Convergence of identified linear density; (b) convergence of identified linear density; (c) convergence of identified linear stiffness  $k_1$ ; (d) convergence of identified linear stiffness  $k_6$ ; (e) convergence of identified damping coefficient  $a_1$ ; (f) convergence of identified damping coefficient  $a_2$ .

The parameter identification values, true values and identified relative error of all elements are listed in Table 1. It is shown that all the elements' parameter identification results meet the accuracy requirements; the relative error of the identified mass, stiffness and damping coefficients relative to their true value is less than 5%.

**Table 1.** The parameters identification results of the simply supported beam.

Parameter	Identified	Actual	Relative Error (%)
$k_1$ (KN.m)	4.675	4.828	−2.60
$k_2$ (KN.m)	4.908	4.828	2.25
$k_3$ (KN.m)	5.015	4.828	3.87
$k_4$ (KN.m)	4.626	4.828	−4.18
$k_5$ (KN.m)	4.628	4.828	−4.17
$k_6$ (KN.m)	4.962	4.828	2.77
$\bar{m}_1$ (kg/m)	6.140	5.850	4.95
$\bar{m}_2$ (kg/m)	5.727	5.850	−2.10
$\bar{m}_3$ (kg/m)	5.765	5.850	−1.45
$\bar{m}_4$ (kg/m)	5.993	5.850	2.44
$\bar{m}_5$ (kg/m)	5.724	5.850	−2.15
$\bar{m}_5$ (kg/m)	6.075	5.850	3.67
$a_1$	1.380	1.356	1.77
$a_2 (1 \times 10^{-3})$	1.206	1.179	2.29



### 3.2. Identification of a Plane Frame Structure Subjected to Stationary Filtered White Noise Excitation

In order to further verify the effectiveness of the proposed algorithm for the joint state-parameter identification of the structure with a non-diagonal mass matrix under unknown mass, a plane frame shown in Figure 4 is investigated in this case. A one-story two-span plane span was applied here for numerical simulation. All beams and columns adopt a consistent mass matrix and consistent stiffness matrix; the mass and stiffness matrix detailed representation are shown in Appendix B. Rayleigh damping is assumed in this numerical simulation case. The bases are assumed to be fixed. Therefore, the plane frame contains a total of 12 DOFS, and each node point has three degrees of freedom (horizontal, vertical and rotational).

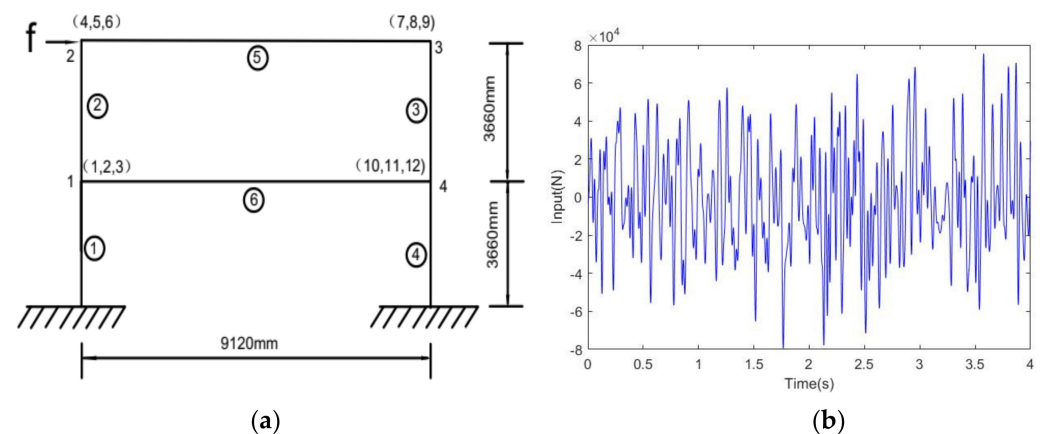


**Figure 4.** A plane frame subjected to stationary filtered white noise excitation. (a) A plane frame subjected to external excitation; (b) filtered white noise excitation generated according to the Kanai–Tajimi power spectrum.

In this numerical example, the height of the column is 3.66 m and the length of the beam is 9.12 m. The Young’s modulus and material density are taken as 206 GPa and 7850 kg/m<sup>3</sup>, respectively. The first two natural frequencies obtained from the plane frame model are 7.55 Hz and 27.3 Hz. A modal damping ratio of 5% is assumed for the first two modes.

Structural parameters are selected as follows: The cross-section area and moment of inertia of each element are  $A_i = 2.68 \times 10^{-2} \text{ m}^2$  and  $I_{zi} = 4.870 \times 10^{-4} \text{ m}^4$  ( $i = 1, 2 \dots 6$ ). The linear stiffness of each column element is  $k_i = \frac{EI_{zi}}{l_i} = 27,410 \text{ KN.m}$  ( $i = 1, 2, 3, 4$ ), linear stiffness of each beam element is  $k_i = \frac{EI_{zi}}{l_i} = 11,000 \text{ KN.m}$  ( $i = 5, 6$ ). All the beams and columns adopt uniform linear density  $\bar{m}_i = \rho_i A_i = 210.38 \text{ kg/m}$  ( $i = 1, 2 \dots 6$ ). The Rayleigh damping coefficients were calculated to be  $a_1 = 3.738$  and  $a_2 = 4.538 \times 10^{-4}$  according to the first two nature frequencies. The initial guess values for the identified parameters are selected as:  $k_{i,0} = 21,928 \text{ KN.m}$  ( $i = 1, 2 \dots 4$ ),  $k_{i,0} = 8800 \text{ KN.m}$  ( $i = 5, 6$ ),  $\bar{m}_{i,0} = 166.3 \text{ Kg/m}$  ( $i = 1, 2 \dots 6$ ),  $a_{1,0} = 2.990$ ,  $a_{2,0} = 3.630$ .

In order to verify the robustness of the algorithm to external excitation, this case adopts the filtered stationary white noise excitation generated according to the Kanai–Tajimi power spectrum as the external excitation [33].

$$S_{\dot{x}_g}(\omega) = \frac{\omega_g^4 + 4\zeta_g^2 \omega_g^2 \omega^2}{(\omega^2 - \omega_g^2)^2 + 4\zeta_g^2 \omega_g^2 \omega^2} S_0 \quad (19)$$

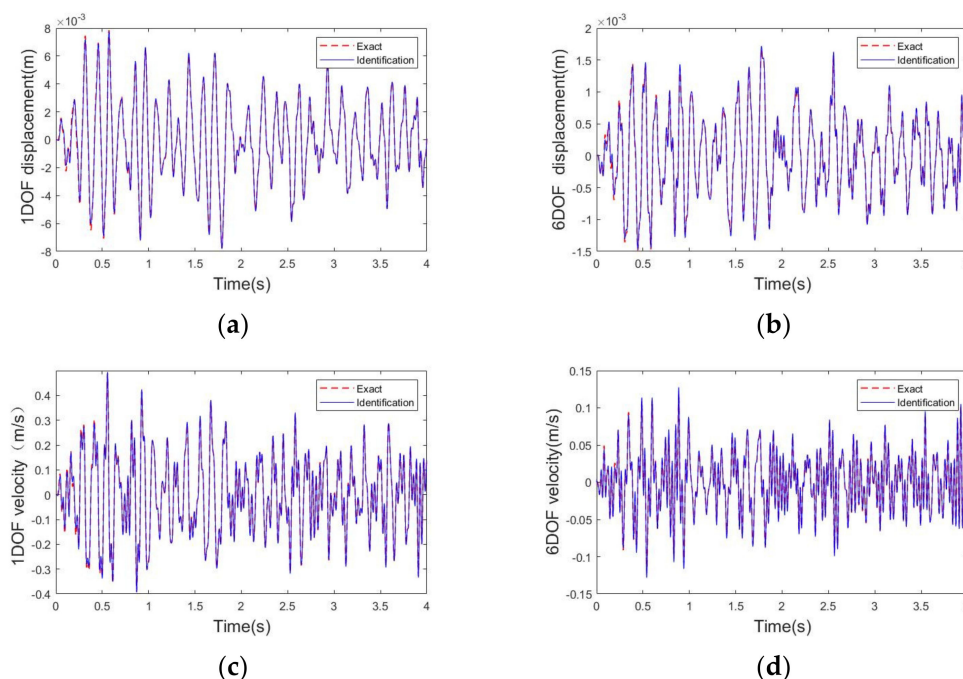
where  $S_0$  is the input white noise spectral density,  $\omega_g$  and  $\zeta_g$  are the characteristic frequency and characteristic damping ratio of the site, respectively. In this case, these parameters were taken as  $\omega_g = 15.6 \text{ (rad/s)}$ ,  $\zeta_g = 0.6$ . In this study, the stationary filtered white noise time history generated according to the Kanai–Tajimi power spectrum was chosen as the

external excitation acting at 4thDOF. From the finite element model built in matlab, the acceleration, velocity and displacement responses of the structure are obtained by solving differential Equation (17) using the 4th-order Ronge–Kutta integration method.

Suppose eight accelerometers are mounted on the plane frame to measure the horizontal accelerations at 1,2,3 and 4 nodal points, i.e.,  $(\ddot{x}_1, \ddot{x}_4, \ddot{x}_7, \ddot{x}_{10})$ , two vertical accelerations at 1,4 nodal points, i.e.,  $(\ddot{x}_2, \ddot{x}_{11})$ , and two rotational accelerations at 1,4 nodal points, i.e.,  $(\ddot{x}_3, \ddot{x}_{12})$ . It is usually a good approximation to assume the rotational motion is related to horizontal motion through the static deflection relation; hence, we compute the rotational acceleration  $\ddot{x}_3$  and  $\ddot{x}_{12}$  from the horizontal acceleration  $\ddot{x}_1$  at node 1. Consequently, our measured response vector is  $y = [\ddot{x}_1, \ddot{x}_2, \ddot{x}_3, \ddot{x}_4, \ddot{x}_7, \ddot{x}_{10}, \ddot{x}_{11}, \ddot{x}_{12}]^T$ .

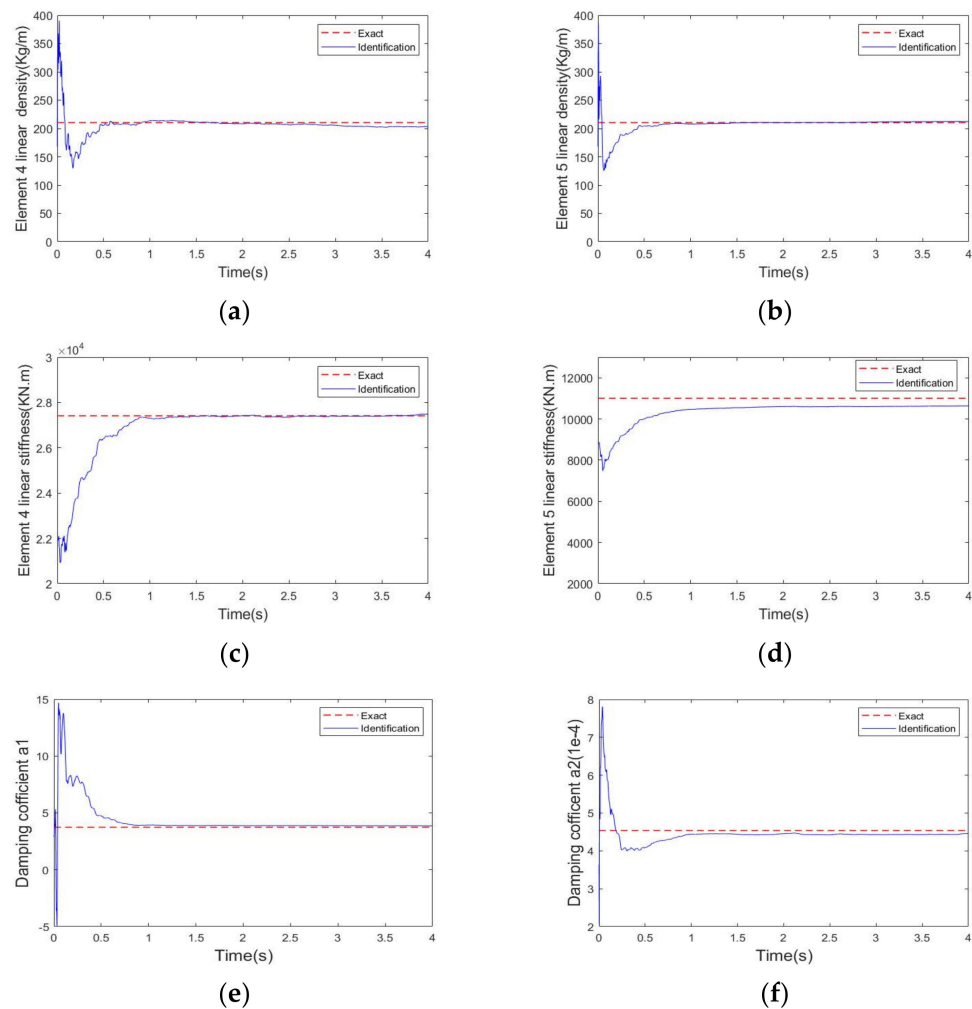
When considering the existence of measurement noise, a Gaussian white sequence with a 1% root-mean-square noise-to-signal ratio was added to the calculated response. The sampling frequency is 1024 Hz, and the sampling time is 4 s.

Figure 5a,b show the comparisons of the identified and exact time histories of Horizontal displacement ( $z_1$ ) of nodal 1 and rotational displacement ( $z_6$ ) of nodal 4. The identified time histories and the exact time histories  $\dot{z}_1, \dot{z}_6$ , are depicted in Figure 5c,d, respectively. It is shown that both structural displacement and velocity responses can be identified effectively.



**Figure 5.** Comparisons of the exact and identified displacements and velocities. (a) Comparison of the exact and identified  $z_1$ ; (b) comparison of the exact and identified  $z_6$ ; (c) comparison of the exact and identified  $\dot{z}_1$ ; (d) comparison of the exact and identified  $\dot{z}_6$ .

The convergence of six parameters  $(\bar{m}_4, \bar{m}_5, k_4, k_5, a_1, a_2)$  is demonstrated in Figure 6. It shows that the identified linear density of element 4 ( $\bar{m}_4$ ) and element 5 ( $\bar{m}_5$ ), the identified linear stiffness of element 4 ( $k_4$ ) and element 5 ( $k_5$ ), and the dumping coefficients  $a_1, a_2$  can be identified effectively. Table 2 provides all the elements' parameter identification values, true values and identified relative error of all elements. It is shown that all the elements' parameter identification results meet the accuracy requirements and the relative error of the identified mass, stiffness and damping coefficients relative to their true value is less than 5%.



**Figure 6.** Parameter estimation results for the plane frame. (a) Convergence of identified linear density  $\bar{m}_4$ ; (b) convergence of identified linear density  $\bar{m}_5$ ; (c) convergence of identified linear stiffness  $k_4$ ; (d) convergence of identified linear stiffness  $k_5$ ; (e) convergence of identified damping coefficient  $a_1$ ; (f) convergence of identified damping coefficient  $a_2$ .

**Table 2.** The parameters identification results of the plane frame.

Parameter	Identified	Actual	Relative Error (%)
$k_1$ (KN.m)	27,800	27,410	1.42
$k_2$ (KN.m)	27,906	27,410	1.81
$k_3$ (KN.m)	28,434	27,410	3.73
$k_4$ (KN.m)	27,484	27,410	0.27
$k_5$ (KN.m)	10,635	11,000	−3.32
$k_6$ (KN.m)	10,740	11,000	−2.36
$\bar{m}_1$ (kg/m)	216.612	210.380	2.96
$\bar{m}_2$ (kg/m)	204.300	210.380	−2.89
$\bar{m}_3$ (kg/m)	211.701	210.380	0.63
$\bar{m}_4$ (kg/m)	203.171	210.380	−3.42
$\bar{m}_5$ (kg/m)	212.021	210.380	0.80
$\bar{m}_6$ (kg/m)	206.901	210.380	−1.65
$a_1$	3.851	3.738	3.02
$a_2 (1 \times 10^{-4})$	4.456	4.538	−1.80

#### 4. Conclusions

In this paper, a joint state-parameter identification algorithm based on UKF was provided for a structure with unknown mass using partial acceleration measurements. Numerical verification was performed using a simply supported beam subjected to broadband white noise excitation and a one-span two-story plane frame subjected to filtered white noise excitation generated according to the Kanai–Tajimi power spectrum. The conclusions are as follows:

1. Numerical results indicate that the proposed approach can effectively identify the state and unknown parameters, including mass, stiffness, and damping coefficients of non-chain-like structures;
2. Unlike some existing methods, the proposed identification algorithm does not require iterative estimation at each time step, which makes the approach suitable for real-time identification;
3. The proposed algorithm for the identification of joint state-parameter is effective in a noisy environment. In this study, with reasonable noise included, the identification results for structural stiffness, damping and mass are robust to the measurement noises.

In summary, the proposed algorithm is suitable for the real-time identification of states and parameters of a structure with a non-diagonal mass matrix under unknown mass using partial acceleration measurement. Therefore, this paper provides a promising way for the joint state-parameter identification of non-chain-like structures with unknown mass information. However, this paper only demonstrates the algorithm for the identification of linear structures with a non-diagonal mass matrix and assumes that the external excitation is measurable. Extensions of such identification studies are conducted by the authors.

**Author Contributions:** S.W.: Writing—review, Investigation, Software, Data curation, Validation. Y.L.: Conceptualization, Methodology, Supervision. All authors have read and agreed to the published version of the manuscript.

**Funding:** The National Natural Science Foundation of China through the project No. 52178304.

**Data Availability Statement:** All data, models and code generated or used in this study are available from the corresponding author upon reasonable request.

**Conflicts of Interest:** The authors declare no conflict of interest.

#### Appendix A. The Local Mass and Stiffness Matrices

The local mass and stiffness matrices of the  $i$ -th element of the 2D simply supported beam can be expressed as:

$$\mathbf{M}_i = \frac{\bar{m}_i l_i}{420} \begin{bmatrix} 156 & 22l_i & 54 & -13l_i \\ 22l_i & 4l_i^2 & 13l_i & 13l_i \\ 54 & 13l_i & 156 & -22l_i \\ -13l_i & -3l_i^2 & -22l_i & 4l_i^2 \end{bmatrix} \quad (\text{A1})$$

$$\mathbf{K}_i = k_i \begin{bmatrix} 12/l_i^2 & 6/l_i & -12/l_i^2 & 6/l_i \\ 6/l_i & 4 & -6/l_i & 2 \\ -12/l_i^2 & -6/l_i & 12/l_i^2 & -6/l_i \\ 6/l_i & 2 & -6/l_i & 4 \end{bmatrix} \quad (\text{A2})$$

where mass is uniform along the length of the member, and its mass distribution along the length is defined by the linear density  $\bar{m}_i$ . The stiffness parameter of the  $i$ -th member is defined by the line stiffness  $k_i = \frac{EI_{zi}}{l_i}$ , in which  $E$ ,  $I_{zi}$ ,  $l_i$  represent Young's Modulus, inertia moment, and element length, respectively.

## Appendix B. The Local Mass and Stiffness Matrices

The local mass and stiffness matrices of the  $i$ -th element of the 2D plane frame can be expressed as:

$$\mathbf{M}_i = \frac{\bar{m}_i l_i}{420} \begin{bmatrix} 140 & 0 & 0 & 70 & 0 & 0 \\ 0 & 156 & 22l_i & 0 & 54 & -13l_i \\ 0 & 22l_i & 4l_i^2 & 0 & 13l_i & -3l_i^2 \\ 70 & 0 & 0 & 140 & 0 & 0 \\ 0 & 54 & 13l_i & 0 & 156 & -22l_i \\ 0 & -13l_i & -3l_i^2 & 0 & -22l_i & 4l_i^2 \end{bmatrix} \quad (\text{A3})$$

$$\mathbf{K}_i = k_i \begin{bmatrix} A_i/I_{zi} & 0 & 0 & -A_i/I_{zi} & 0 & 0 \\ 0 & 12/l_i^2 & 6/l_i & 0 & -12/l_i^2 & 6/l_i \\ 0 & 6/l_i & 4 & 0 & -6/l_i & 2 \\ -A_i/I_{zi} & 0 & 0 & A_i/I_{zi} & 0 & 0 \\ 0 & -12/l_i^2 & -6/l_i & 0 & 12/l_i^2 & -6/l_i \\ 0 & 6/l_i & 2 & 0 & -6/l_i & 4 \end{bmatrix} \quad (\text{A4})$$

where mass is uniform along the length of the member, and its mass distribution along the length is defined by the linear density  $\bar{m}_i$ . The stiffness parameter of the  $i$ -th member is defined by the line stiffness  $k_i = \frac{EI_{zi}}{l_i}$ , in which  $E$ ,  $I_{zi}$ ,  $l_i$  represent Young's Modulus, inertia moment and element length, respectively. The cross-sectional area is represented by  $A_i$ .

## References

- Hwang, J.S.; Kwon, D.K.; Kareem, A. Frequency Domain State Space-Based Mode Decomposition Framework. *J. Eng. Mech.* **2019**, *145*, 04019051. [[CrossRef](#)]
- Roy, K.; Ray-Chaudhuri, S. Fundamental mode shape and its derivatives in structural damage localization. *J. Sound Vib.* **2013**, *332*, 5584–5593. [[CrossRef](#)]
- Santos, F.; Cismasiu, C.; Cismasiu, I.; Bedon, C. Dynamic Characterisation and Finite Element Updating of a RC Stadium Grandstand. *Buildings* **2018**, *8*, 141. [[CrossRef](#)]
- Sivasuriyan, A.; Vijayan, D.S.; Górski, W.; Wodzyński, L.; Vaverková, M.D.; Koda, E. Practical Implementation of Structural Health Monitoring in Multi-Story Buildings. *Buildings* **2021**, *11*, 263. [[CrossRef](#)]
- Chaudhary, P.K.; Anjneya, K.; Roy, K. Fundamental Mode Shape-Based Structural Damage Quantification Using Spectral Element Method. *J. Eng. Mech.* **2021**, *147*, 04021091. [[CrossRef](#)]
- Tamuly, P.; Chakraborty, A.; Das, S. Simultaneous Input and Parameter Estimation of Hysteretic Structural Systems Using Quasi-Monte Carlo-Simulation-Based Minimum Variance Unbiased Estimator. *J. Bridge Eng.* **2021**, *26*, 04021081. [[CrossRef](#)]
- Astroza, R.; Ebrahimian, H.; Li, Y.; Conte, J.P. Bayesian nonlinear structural FE model and seismic input identification for damage assessment of civil structures. *Mech. Syst. Signal Process.* **2017**, *93*, 661–687. [[CrossRef](#)]
- Erazo, K.; Nagarajaiah, S. Bayesian structural identification of a hysteretic negative stiffness earthquake protection system using unscented Kalman filtering. *Struct. Control Health Monit.* **2018**, *25*, e2203. [[CrossRef](#)]
- Ebrahimian, H.; Astroza, R.; Conte, J.P.; Papadimitriou, C. Bayesian optimal estimation for output-only nonlinear system and damage identification of civil structures. *Struct. Control Health Monit.* **2018**, *25*, e2128. [[CrossRef](#)]
- Krishnan, M.; Bhowmik, B.; Hazra, B.; Pakrashi, V. Real time damage detection using recursive principal components and time varying auto-regressive modeling. *Mech. Syst. Signal Process.* **2018**, *101*, 549–574. [[CrossRef](#)]
- Yuan, P.; Wu, Z.F.; Ma, X.R. Estimated mass and stiffness matrices of smear building from modal test data. *Earthq. Eng. Struct. Dyn.* **1998**, *27*, 415–421. [[CrossRef](#)]
- Chakraverty, S. Identification of structural parameters of multistory shear buildings from modal data. *Earthq. Eng. Struct. Dyn.* **2005**, *34*, 543–554. [[CrossRef](#)]
- Mukhopadhyay, S.; Lus, H.; Betti, R. Modal parameter based structural identification using input-output data: Minimal instrumentation and global identifiability issues. *Mech. Syst. Signal Process.* **2014**, *45*, 283–301. [[CrossRef](#)]
- Mukhopadhyay, S.; Lus, H.; Betti, R. Structural identification with incomplete output-only data and independence of measured information for shear-type systems. *Earthq. Eng. Struct. Dyn.* **2016**, *45*, 273–296. [[CrossRef](#)]
- Zhang, J.; Xu, J.C.; Guo, S.L.; Wu, Z.S. Flexibility-based structural damage detection with unknown mass for IASC-ASCE benchmark studies. *Eng. Struct.* **2013**, *48*, 486–496. [[CrossRef](#)]
- Farshadi, M.; Esfandiari, A.; Vahedi, M. Structural model updating using incomplete transfer function and modal data. *Struct. Control. Health Monit.* **2016**, *24*, e1932. [[CrossRef](#)]
- Mustafa, S.; Matsumoto, Y. Bayesian Model Updating and Its Limitations for Detecting Local Damage of an Existing Truss Bridge. *J. Bridge Eng.* **2017**, *22*, 04017019. [[CrossRef](#)]

18. Zeng, J.; Kim, Y.H. Identification of Structural Stiffness and Mass using Bayesian Model Updating Approach with Known Added Mass: Numerical Investigation. *Int. J. Struct. Stab. Dyn.* **2020**, *20*, 2050123. [[CrossRef](#)]
19. Mei, Q.P.; Gul, M. Novel Sensor Clustering-Based Approach for Simultaneous Detection of Stiffness and Mass Changes Using Output-Only Data. *J. Struct. Eng.* **2015**, *141*, 04014237. [[CrossRef](#)]
20. Do, N.T.; Gul, M. A time series based damage detection method for obtaining separate mass and stiffness damage features of shear-type structures. *Eng. Struct.* **2020**, *208*, 09914. [[CrossRef](#)]
21. Masri, S.F.; Bekey, G.A.; Sassti, H. Non-parametric identification of a class of nonlinear multi-degree dynamic systems. *Earthq. Eng. Struct. Dyn.* **1982**, *10*, 1–30. [[CrossRef](#)]
22. Nayeri, R.D.; Masri, S.F.; Ghanem, R.G.; Nigbo, R.L. A novel approach for the structural identification and monitoring of a full-scale 17-story building based on ambient vibration measurements. *Smart Mater. Struct.* **2008**, *17*, 025006. [[CrossRef](#)]
23. Zhan, C.; Lin, D.S.; Li, H.N. A local damage detection approach based on restoring force method. *J. Sound Vib.* **2014**, *333*, 4942–4959. [[CrossRef](#)]
24. Nayeri, R.D.; Tasbihgoo, F.; Wahbeh, M.; Caffrey, G.P.; Masri, S.F.; Conte, J.P.; Elgamal, A. Study of Time-Domain Techniques for Modal Parameter Identification of a Long Suspension Bridge with Dense Sensor Arrays. *J. Eng. Mech.* **2009**, *135*, 669–683. [[CrossRef](#)]
25. Xu, B.; He, J.; Dyke, S.J. Model-free nonlinear restoring force identification for SMA dampers with double Chebyshev polynomials: Approach and validation. *Nonlinear Dyn.* **2015**, *82*, 1507–1522. [[CrossRef](#)]
26. Huang, X.H.; Dyke, S.J.; Sun, Z.X.; Xu, Z.D. Simultaneous identification of stiffness, mass, and damping using an on-line model updating approach. *Struct. Control Health Monit.* **2017**, *24*, e1892. [[CrossRef](#)]
27. Reina, G.; Paiano, M.; Blanco-Claraco, J.L. Vehicle parameter estimation using a model-based estimator. *Mech. Syst. Signal Process.* **2017**, *87*, 227–241. [[CrossRef](#)]
28. Boada, B.L.; Boada, M.J.L.; Zhang, H. Sensor Fusion Based on a Dual Kalman Filter for Estimation of Road Irregularities and Vehicle Mass Under Static and Dynamic Conditions. *IEEE/ASME Trans. Mechatron.* **2019**, *24*, 1075–1086. [[CrossRef](#)]
29. Lei, Y.; Qiu, H.; Zhang, F.B. Identification of structural element mass and stiffness changes using partial acceleration responses of chain-like systems under ambient excitations. *J. Sound Vib.* **2020**, *488*, 115678. [[CrossRef](#)]
30. Zhang, D.Y.; Li, H. Loop substructure identification for shear structures of unknown structural mass using synthesized references. *Smart Mater. Struct.* **2017**, *26*, 085046. [[CrossRef](#)]
31. Zhang, D.Y.; Niu, Z.F.; Tian, J.D.; Li, H. Decentralized loop substructure identification for shear structures with virtual control system. *Struct. Control Health Monit.* **2021**, *29*, e2866. [[CrossRef](#)]
32. Xu, B.; Li, J.; Dyke, S.J.; Deng, B.C.; He, J. Nonparametric identification for hysteretic behavior modeled with a power series polynomial using EKF-WGI approach under limited acceleration and unknown mass. *Int. J. Non-Linear Mech.* **2020**, *119*, 103324. [[CrossRef](#)]
33. Song, W. Generalized minimum variance unbiased joint input-state estimation and its unscented scheme for dynamic systems with direct feedthrough. *Mech. Syst. Signal Process.* **2018**, *99*, 886–920. [[CrossRef](#)]